Optically-Pumped Magnetometers for MEG

Svenja Knappe, Tilmann Sander and Lutz Trahms

Abstract Optically-pumped magnetometers (OPMs) have seen rapid progress over the last decade in terms of performance and technology development. As highly sensitive room-temperature magnetometers they present several advantages over superconducting quantum interference device (SQUID) sensors, such as the possibility for conformal geometries and low-maintenance systems. We review the state of the art and different types of low-field OPMs, as well as the first magnetoencephalography (MEG) demonstrations with OPMs. Several challenges remain, such as the demonstration of OPM multichannel systems, their limited dynamic range, and the demonstration of gradiometric operation to name just a few. Certainly OPMs present a promising technology to complement existing SQUID-based installations.

Keywords Optically pumped magnetometer · Magnetoencephalography · Superconducting quantum interference device · Magnetocardiography · Multichannel · Electron spin resonance · Micro-electromechanical system · Alkali-metal vapor cell · Atomic magnetometer · Optical magnetometer

1 Introduction

Rapid advances in atomic physics over the last decade have led to the design of optical magnetometers Optically Pumped Magnetometer (OPM) capable of recording biomagnetic signals; although the first attempts are much older (Livanov

S. Knappe (✉)
National Institute of Standards and Technology, Boulder, CO 80303, USA
e-mail: Svenja.knappe@nist.gov

T. Sander · L. Trahms
Physikalisch-Technische Bundesanstalt, 10587 Berlin, Germany

S. Supek and C. J. Aine (eds.), *Magnetoencephalography*,
DOI: 10.1007/978-3-642-33045-2_49,

et al. 1981). Further motivation to develop room-temperature alternatives to low-temperature SQUID magnetometers comes from the spiraling helium costs, which complicate the operation of MEG systems. Optical magnetometers have demonstrated sensitivities similar to those of the best SQUID magnetometers (Deng et al. 2010), at least over a narrow frequency band. At present, only laboratory prototypes of OPMs exist, and few MEG measurements have been demonstrated (Xia et al. 2006; Johnson et al. 2010; Sander, et al. 2012). Clearly these OPMs cannot compete with sophisticated commercial SQUID-based MEG systems yet. Nevertheless, OPMs have the potential to complement SQUID-based systems or to replace them for certain applications. This might soon be the case in magnetocardiography, where multi-channel OPM systems have been implemented (Bison et al. 2009; Wyllie et al. 2012). Other applications of OPMs that have been demonstrated include magnetic resonance imaging (Xu et al. 2006; Savukov et al. 2009) and magnetic relaxation measurements of nano-particles (Knappe et al. 2010).

OPMs are individually placeable room-temperature sensors, which entail several advantages. First, without the need for a dewar, OPMs allow for a shorter distance between sensor and scalp. This will enhance the MEG signal strength at the location of the sensor, especially for sources at shallow depths beneath the skull and can therefore result in a higher signal-to-noise ratio. Second, sensor placement conformal to the individual scalp reduces the distance between sensor and source further, which can be especially advantageous for MEG measurements on children and for flexible research systems. This would require, however, accurate detection of the sensor arrangement for analysis purposes. Third, open geometries and room-temperature operation simplify the combination with other modalities, such as electroencephalography (EEG) or functional near-infrared spectroscopy in the same system. Fourth, the operation of OPMs does not require a shielded room for the measurements, although the practicability of biomagnetic measurements with OPMs in an unshielded environment still must be demonstrated.

These advantages, nevertheless, come at a price. The OPMs used for MEG so far have much smaller dynamic ranges and bandwidths compared to those of SQUIDs. Furthermore, gradiometers with good common-mode rejection ratios have not yet been demonstrated; cross-talk issues with neighboring sensors need to be resolved, and multichannel devices need to be demonstrated.

2 Principle of Operation

The OPMs used for MEG recordings so far use electron-spin resonances in alkali atoms in the vapor phase. These atoms have a single valence electron that determines most of the properties of interest. Due to their electron spin and magnetic moment, the spin precesses around a magnetic field at a well-defined frequency, the Larmor frequency (see Fig. 1). Furthermore, a large macroscopic

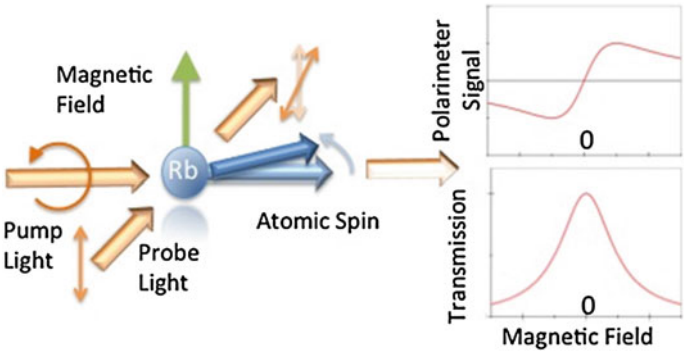

Fig. 1 Light from a circularly polarized laser beam optically pumps the Rb atoms, while light from a second laser beam probes the magnetic field-dependent spin orientation through polarization rotation. Both the transmission and polarimeter signal show a resonance as a function of magnetic field

polarization can be produced in these atoms through optical pumping (Happer 1972). In its simplest form, the spin from near-resonant circularly polarized photons is transferred to the atoms during absorption. Since these incident photons all have spins in a specific direction, the spins of the atoms become oriented. This process is very efficient, and can achieve atomic spin-polarizations close to unity. A magnetic field changes the atomic spin orientation, which can be probed once again with near-resonant light, making use of the absorption or dispersion of the light. The light carries information about the external magnetic field.

For MEG measurements made thus far, only zero-field magnetometers have been used. When operated in a regime of frequent atomic collisions and in low magnetic fields, the decoherence mechanism through spin-exchange collisions can be suppressed (Happer and Tang 1973). This so-called spin-exchange relaxation-free (SERF) regime (Allred et al. 2002) allows for very high magnetometer sensitivities, but limits the dynamic range of the magnetometer. In very small magnetic fields, the spins are tilted by the magnetic field and a static reorientation results from the balance between precession and continuous pumping. Again, the orientation of the spins is measured with near-resonant light by detecting the transmission of resonant light. Often it is more advantageous to monitor the polarization rotation of a slightly detuned light beam, which is usually done with a balanced polarimeter. This method can cancel intensity noise of the laser light and also tolerate much higher optical thickness of the vapor, since the light is detuned from resonance. In order to increase the signal-to-noise ratio, phase-sensitive detection can be implemented. For the zero-field resonances, one parameter, such as the magnetic field or the probe light polarization, is modulated and the same frequency component of the light is detected at a fixed phase with the modulation. Typically, OPMs measure the magnitude of the magnetic field, but the zero-field OPMs used for MEG are operated to measure a magnetic-field component in a certain direction, e.g., through external field modulation with an additional Helmholtz coil pair.

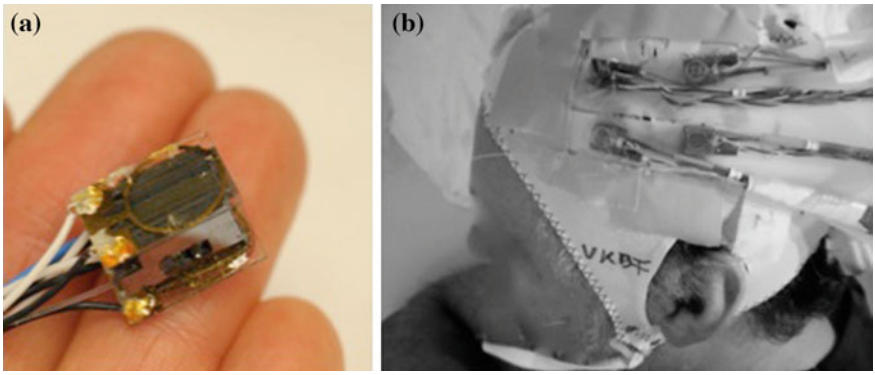

Fig. 2 **a** Photograph of a chip-scale OPM sensor head. **b** Photograph of four chip-scale OPMs attached to an EEG cap for MEG measurements. The fibers and wires needed to drive a sensor are collected in a bundle leaving the head tangentially

All of the devices used for MEG demonstrations have been operated in an open-loop configuration, where the dynamic range was limited by the linewidth of the resonance to below 100 nT. While feedback systems have been demonstrated in principle, they have not yet reached the same sensitivities (Seltzer and Romalis 2004). Furthermore, the response of the magnetometer shows the behavior of a first-order low-pass filter with a width corresponding to the linewidth of the atomic resonance. This usually limits the intrinsic bandwidth to below 1 kHz.

Figure 2a shows a chip-scale high-sensitivity OPM, which was manufactured by use of a micro-electro-mechanical-system (MEMS) process (Mhaskar et al. 2012). In the center of the cube is an alkali-vapor cell, heated to generate a sufficient atomic density of the vapor (Knappe et al. 2005). A laser, on resonance with a transition of the atoms, is circularly polarized and optically pumps the atoms. The same laser is used to monitor the atomic polarization by detecting the transmitted light with a photodiode (Dupont-Roc et al. 1969; Shah et al. 2007). This is only one of many possible configurations with respect to polarization, sensor shape, and beam.

3 MEG with OPMs

Three different demonstrations of MEG measurements with OPMs on human subjects have been published to this date. In the first one, Xia et al. used a $(7.5\ \text{cm})^3$ Pyrex cell filled with potassium vapor and heated to 180° C (Xia et al. 2006). It was placed on the left side of the head at a distance of 6.25 cm between the scalp and center of the cell. The atoms were polarized with 500 mW circularly polarized pump light, and the magnetic field was monitored through the polarization rotation of linearly polarized probe light at a right angle, so that the OPM

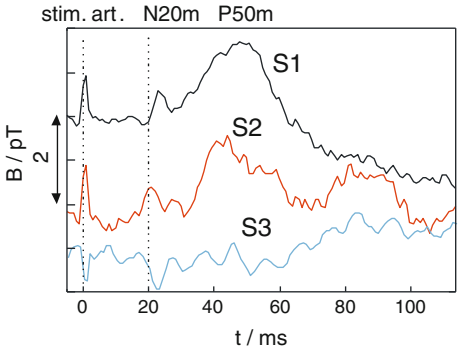

Fig. 3 Exemplary single-channel OPM recordings of the N20 and P50 m brain responses from three subjects (S1–S3). Electrical stimuli were applied to the right median nerve and a total of 5,000 responses were recorded inside a seven-layer magnetically-shielded room. The averaged responses show the stimulus artifact at 0 ms, the N20 m response (20 ms poststimulus), and the P50 m at 50 ms (figure reprinted with permission from Sander et al. 2012, copyright OSA 2012)

was sensitive to the component of the magnetic field normal to the scalp. The probe light was detected by a 16 × 16 photodiode array and 256 parallel channels of roughly 0.4 × 0.4 × 7.5 cm and spacing of 5 mm could be monitored simultaneously. Auditory evoked fields were recorded and the N100 m peak was clearly visible in the data. Six subjects were measured.

In the second paper Johnson et al. demonstrated an OPM with a fiber-coupled sensor head. Pump and probe beams were collinear and passed through a cylindrical Rb vapor cell of diameter 2.5 cm and length 2.5 cm (Johnson et al. 2010). A balanced polarimeter consisted of a photodiode and a quadrant detector, which allowed them to monitor four channels with a spatial distance of 5 mm simultaneously. The distance between cell and scalp was 2 cm, and one component of the magnetic field tangential to the scalp was measured. Evoked fields were recorded after auditory stimulation and after electrical stimulation of the median nerve in a male subject. They were verified by consecutive SQUID measurements.

The third MEG measurement was performed with a fiber-coupled chip-scale OPM (Sander et al. 2012). Here, the Rb vapor cell was of size $(2\ \text{mm})^3$ and the magnetometer was operated with a single laser beam and detection of the transmitted light. The distance to the scalp was 4 mm and the sensor was attached to an EEG cap for ease of placement similar to the four-channel configuration shown in Fig. 2b. The magnetic field component normal to the scalp was measured in three subjects. The sensor was operated with a modulation field of 1.8 kHz and the high-frequency cutoff was optimized to achieve a bandwidth sufficient for the recording of brain signals. By use of a coil to generate an AC magnetic field, it was verified that the − 3 dB cut-off for the sensor was at 150 Hz. This is sufficient to resolve the evoked responses N20 and P50 m due to electrical stimulation of the median nerve at the wrist, as can be seen in the typical MEG results shown in Fig. 3. The same responses in the same subjects were identified in consecutive SQUID measurements.

An OPM very similar to the one used in Xia et al. was demonstrated to measure signals from a dipolar current source immersed in a saline solution MEG phantom (Taue et al. 2010). A $(3\ \mathrm{cm})^3$ potassium cell was used to record the magnetic field at several locations around the phantom with a single channel. From the measured field map the location of the dipolar current source was estimated, and good agreement was obtained with the known position.

4 Conclusions and Outlook

In the last decade several research groups have demonstrated the measurement of MEG signals by use of single OPM sensor units. The head coverage was very limited, but the signals obtained show that OPMs are suitable as MEG sensors. It is still an open question whether multichannel OPM systems will achieve the same sensitivity as the best multichannel SQUID systems with up to 300 sensors. The reduced distance between the cortical source and OPM will certainly allow for stronger signals.

For a rapid advance of OPMs the development focus should be on broadband operation of multichannel devices with self-tuning capabilities. At least two types of multichannel systems appear promising: a standalone multichannel OPM device for weak shielding and a combined SQUID and OPM system for the most demanding studies. A combined system could consist, for example, of a SQUID helmet design with an additional OPM array to cover other positions difficult to reach with a closed dewar, such as the base of the head or the forehead. Development of multichannel devices can utilize experience gathered during the design of multichannel SQUID systems, hopefully reducing development time and cost. On a technical level, OPM gradiometers need to be demonstrated with dynamic ranges high enough to achieve common-mode rejections sufficient to suppress residual magnetic fields fluctuations inside the shielded room. Furthermore, three-axis OPMs would be desirable. It appears sensible to commercialize single-unit OPMs in order that system developers can buy sensors off the shelf to design multichannel systems themselves.

The development of OPMs is accelerated by a current helium shortage, which could also lead to a new generation of closed-cycle refrigeration systems suitable to support SQUID MEG systems. OPMs nevertheless offer the advantage of a flexible geometry, which might allow gathering a more complete picture of brain function (see other chapters in the present book and Brookes and Singh (2013) for more on challenges in MEG research). Overall, OPMs are an attractive candidate for designing inexpensive low-maintenance MEG systems and judging from the initial MEG demonstrations no obvious shortcomings could be identified, which would prevent the successful use of OPMs in large-scale MEG systems.

References

Allred JC, Lyman RN, Kornack TW, Romalis MV (2002) High-sensitivity atomic magnetometer unaffected by spin-exchange relaxation. Phys Rev Lett 89:130801

Bison G, Castagna N, Hofer A, Knowles P, Schenker JL, Kasprzak M, Saudan H, Weis A (2009) A room temperature 19-channel magnetic field mapping device for cardiac signals. Appl Phys Lett 95:173701

Brookes M, Singh K (2013) Methods in mind. Phys World 25:39–44

Dang HB, Maloof AC, Romalis MV (2010) Ultrahigh sensitivity magnetic field and magnetization measurements with an atomic magnetometer. Appl Phys Lett 97:151110

Dupont-Roc J, Haroche S, Cohen-Tannoudji C (1969) Detection of very weak magnetic fields (10–9 gauss) by Rb zero-field level crossing resonances. Phys Lett A 28:628–639

Happer W (1972) Optical pumping. Rev Mod Phys 44:169–249

Happer W, Tang H (1973) Spin-exchange shift and narrowing of magnetic resonance lines in optically pumped alkali vapors. Phys Rev Lett 31:273

Johnson C, Schwindt PDD, Weisend M (2010) Magnetoencephalography with a two-color pump-probe, fiber-coupled atomic magnetometer. Appl Phys Lett 97:243703

Knappe S, Gerginov V, Schwindt PDD, Shah V, Robinson H, Hollberg L, Kitching J (2005) Atomic vapor cells for chip-scale atomic clocks with improved long-term frequency stability,". Opt Lett 30:2351–2353

Knappe S, Sander TH, Kosch O, Wiekhorst F, Kitching J, Trahms L (2010) Cross-validation of microfabricated atomic magnetometers with superconducting quantum interference devices for biomagnetic applications. Appl Phys Lett 97:133703

Livanov MN, Kozolov AN, Sinelnikova SE, Kholodov JA, Markin VP, Gorbach AM, Korinewsky AV (1981) Record of the human magnetocardiogram by the quantum gradiometer with optical pumping. Adv Cardiol 28:78–80

Mhaskar R, Knappe S, Kitching J (2012) A low-power, high-sensitivity micromachined optical magnetometer. Appl Phys Lett 101:241105

Sander TH, Preusser J, Mhaskar R, Kitching J, Trahms L, Knappe S (2012) Magnetoencephalography with a chip-scale atomic magnetometer. Biomed Opt Express 3:981–990

Savukov IM, Zotev VS, Volegov PL, Espy MA, Matlashov AN, Gomez JJ, Kraus RH Jr (2009) MRI with an atomic magnetometer suitable for practical imaging applications. J Mag Resonanace 199:188–191

Seltzer SJ, Romalis MV (2004) Unshielded three-axis vector operation of a spin-exchange-relaxation-free atomic magnetometer. Appl Phys Lett 85:4804–4806

Shah V, Knappe S, Schwindt PDD, Kitching J (2007) Subpicotesla atomic magnetometry with a microfabricated vapour cell. Nat Photonics 1:649–652

Taue S, Sugihara Y, Kobayashi T, Ichihara S, Ishikawa K, Mizutani N (2010) Development of a highly sensitive optically pumped atomic magnetometer for biomagnetic field measurements: a phantom study. IEEE Trans Magn 46:3635–3638

Wyllie R, Kauer M, Wakai RT, Walker TG (2012) Optical magnetometer array for fetal magnetocardiography. Opt Lett 37(12):2247–2249

Xia H, Baranga ABA, Hoffman D, Romalis MV (2006) Magnetoencephalography with an atomic magnetometer. Appl Phys Lett 89:211104

Xu S, Yashchuk VV, Donaldson MH, Rochester SM, Budker D, Pines A (2006) "Magnetic resonance imaging with an optical atomic magnetometer. Proc Natl Acad Sci 103:12668–12671